

Light hadronic physics using domain wall fermions in quenched lattice QCD*

Matthew Wingate^a

^aRIKEN BNL Research Center, Brookhaven National Laboratory, Upton, NY 11973, USA

In the past year domain wall fermion simulations have moved from exploratory stages to the point where systematic effects can be studied with different gauge couplings, volumes, and lengths in the fifth dimension. Results are presented here for the chiral condensate, the light hadron spectrum, and the strange quark mass. We focus especially on the pseudoscalar meson mass and show that, in small volume, the correlators used to compute it can be contaminated to different degrees by topological zero modes. In large volume a nonlinear extrapolation to the chiral limit, e.g. as expected from quenched chiral perturbation theory, is needed in order to have a consistent picture of low energy chiral symmetry breaking effects.

1. INTRODUCTION

The RBC Collaboration has recently reported results based on quenched QCD simulations with domain wall fermions on lattices of various volumes and spacings [1]. This talk summarizes our understanding of the behavior of the pseudoscalar meson mass as a function of input quark mass, scaling of the nucleon–rho mass ratio, and strange quark mass. Another set of quenched simulation results with domain wall fermions have been reported by the CP-PACS Collaboration [2].

2. CHIRAL CONDENSATE

A Dirac operator D which has a well-defined index should lead to a chiral condensate which satisfies the following Banks–Casher relation (for finite volume)

$$-\langle \bar{q}q \rangle = \frac{1}{12V} \frac{\langle |\nu| \rangle}{m} + \frac{m}{12V} \left\langle \sum_{i, \lambda_i \neq 0} \frac{1}{\lambda_i^2 + m^2} \right\rangle \quad (1)$$

where λ_i are eigenvalues of the massless Dirac operator and ν is the index of D . Note that these zero modes are chiral and correspond to units of topological charge in the continuum. In full QCD

*Work done in collaboration with T. Blum, P. Chen, N. Christ, C. Cristian, C. Dawson, G. Fleming, A. Kaehler, X. Liao, G. Liu, C. Malureanu, R. Mawhinney, S. Ohta, G. Siebert, A. Soni, C. Sui, P. Vranas, L. Wu, and Y. Zhestkov (RIKEN/BNL/CU Collaboration)

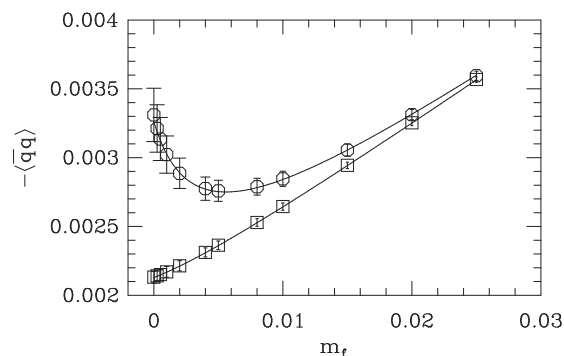


Figure 1. Chiral condensate vs. mass for volumes $8^3 \times 32$ (circles) and $16^3 \times 32$ (squares) at $\beta = 5.7$, $L_s = 32$.

simulations configurations which support eigenvalues equal to zero are suppressed during Monte Carlo updating due to the fermion determinant in the Boltzmann weight. This suppression is absent in the quenched approximation. Consequently, a prominent $1/m$ divergence should appear in $\langle \bar{q}q \rangle$ for quenched simulations in finite volumes. Only when one uses a fermion discretization which admits a non-zero index can one observe this divergence, so the first signal was seen with domain wall fermions [3,4].

Fig. 1 shows $\langle \bar{q}q \rangle$ vs. the input quark mass m_f on two volumes at $\beta = 5.7$ (plaquette gauge action). As expected from Eq. 1 the divergence

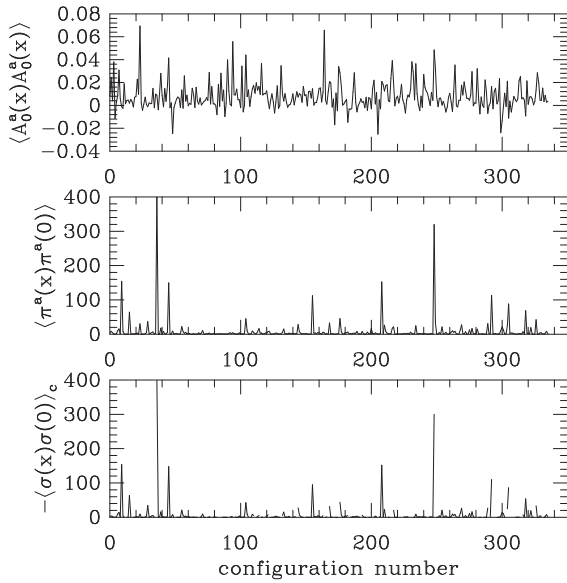


Figure 2. Monte Carlo evolution of correlators on a $8^3 \times 32$ lattice at $\beta = 5.7$ with $L_s = 48$ and $m_f = 0.0$.

is much more severe for the smaller volume, approximately $(1.6 \text{ fm})^3$, than for the larger volume, $\approx (3.2 \text{ fm})^3$. The lines are fits to the form

$$-\langle \bar{q}q \rangle = \frac{a_{-1}}{m_f + \delta m_{\langle \bar{q}q \rangle}} + a_0 + a_1 m_f. \quad (2)$$

$\langle \bar{q}q \rangle$ has a similar divergence on a $(1.6 \text{ fm})^3$ box at $\beta = 6.0$ [1].

3. PSEUDOSCALAR MESON

Given that the chiral condensate in finite volume is sensitive to topological zero modes when using domain wall fermions, we turn to correlators which couple to the pseudoscalar meson, *viz* $\langle A_0^a(x)A_0^a(0) \rangle$ and $\langle \pi^a(x)\pi^a(0) \rangle$. Looking at the spectral decomposition of these correlators [1] leads one to expect the leading zero mode effects to be $\langle A_0^a(x)A_0^a(0) \rangle \propto 1/m$ and $\langle \pi^a(x)\pi^a(0) \rangle \propto 1/m^2$. Indeed time histories of these correlators (Fig. 2) show the latter correlator to be much more singular than the former. Also plotted in Fig. 2 is the connected scalar-scalar correlator

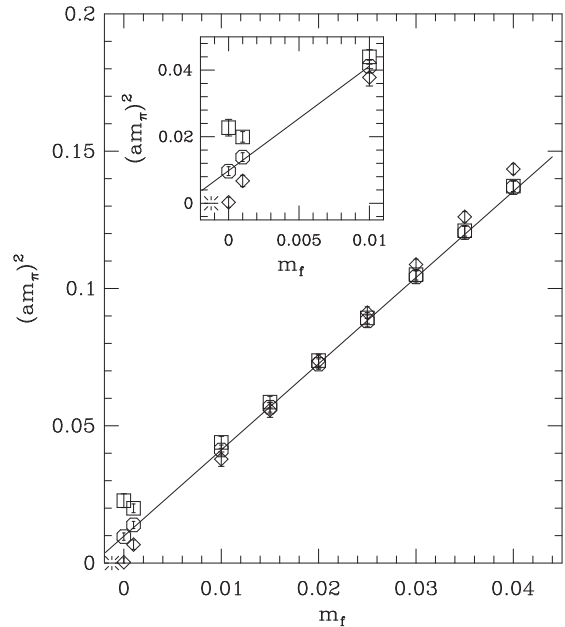


Figure 3. Fits to pseudoscalar meson mass from $\langle \pi^a(x)\pi^a(0) \rangle$ (□), $\langle A_0^a(x)A_0^a(0) \rangle$ (○) and $\langle \pi^a(x)\pi^a(0) \rangle + \langle \sigma(x)\sigma(0) \rangle_c$ (◇) on a $16^3 \times 32$ lattice at $\beta = 6.0$ with $L_s = 16$. The solid line is a linear fit to the circles with $0.01 \leq m_f \leq 0.04$. The asterisk marks m_{res} and the inset magnifies the data at small m_f .

which has the same leading zero mode effects as $\langle \pi^a(x)\pi^a(0) \rangle$, both according to the spectral decomposition and as seen in the data.

The singular behavior of $\langle \pi^a(x)\pi^a(0) \rangle$ for small mass leads to a contamination in the extraction of the meson mass. The mass computed from this correlator is significantly larger at small m_f than the mass computed from $\langle A_0^a(x)A_0^a(0) \rangle$, both at $\beta = 6.0$ (Fig. 3) and at $\beta = 5.7$ (Fig. 4). An attempt can be made to subtract the zero mode effects by extracting a mass from $\langle \pi^a(x)\pi^a(0) \rangle + \langle \sigma(x)\sigma(0) \rangle_c$. At small m_f the fact that the mass from $\langle A_0^a(x)A_0^a(0) \rangle$ is larger than from the “subtracted” correlator could be due to $1/m$ zero mode contributions in $\langle A_0^a(x)A_0^a(0) \rangle$. The subtracted correlator receives increasing contribution from the isovector scalar meson as m_f increases, explaining the deviation of the dia-

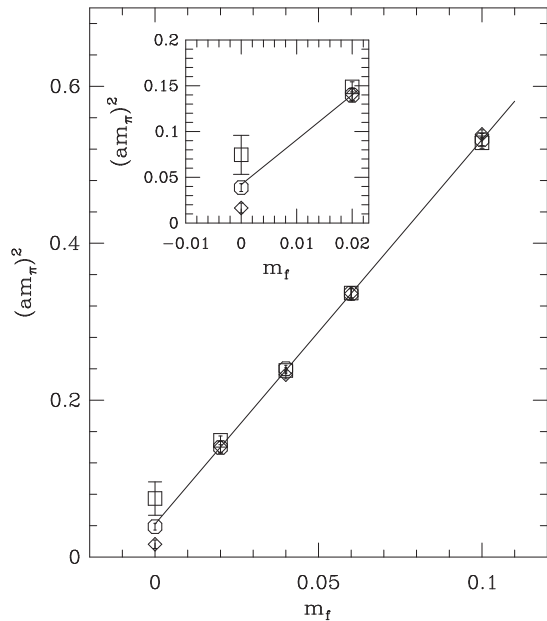


Figure 4. Fits to pseudoscalar meson mass from correlators denoted as in Fig. 3 on a $8^3 \times 32$ lattice at $\beta = 5.7$ with $L_s = 48$. The solid line is a linear fit to the circles with $0.02 \leq m_f \leq 0.1$.

monds for larger values of m_f in Fig. 3.

The zero mode effects disappear within the statistical resolution when the volume is increased. Fig. 5 shows the pseudoscalar meson mass extracted from all three propagators on a lattice with $(3.2 \text{ fm})^3$ spatial volume at $\beta = 5.7$. The asterisk in that figure denotes the residual mass, $m_{\text{res}} = 0.0072(9)$, computed from the ratio of the mid-point pseudoscalar density to the surface pseudoscalar density [1,5]. Although it is not clear on the scale of the plot, the linear extrapolation of $(am_\pi)^2$ to zero in m_f misses m_{res} by over 2σ . Quenched chiral perturbation theory suggests that for vanishing quark mass m , $m_\pi^2 \propto m^{1/(1+\delta)}$ [6]. In order to simplify the fit in the region of m_f where the data points are, one uses

$$(am_\pi)^2 = a_0(m_f + a_1)(1 - \delta \ln(m_f + a_1)). \quad (3)$$

The solid line in Fig. 5 gives $a_1 = 0.0073(10)$, in good agreement with m_{res} , and $\delta = 0.07(4)$. Although the χ^2/dof (with errors estimated from

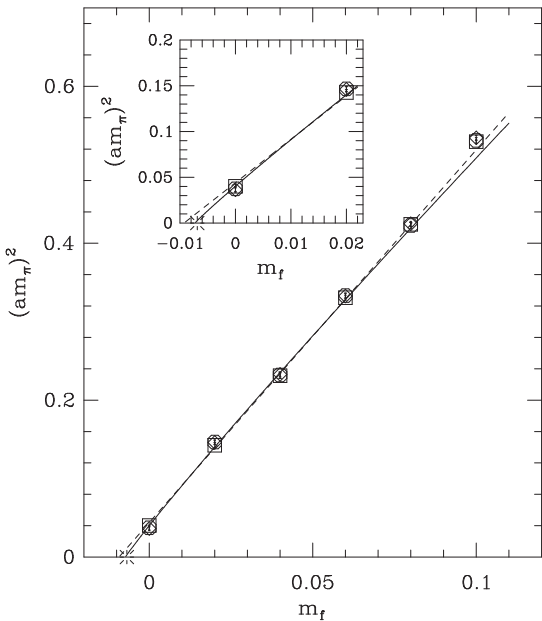


Figure 5. Pseudoscalar meson mass squared vs. m_f on a $16^3 \times 32$ lattice at $\beta = 5.7$ with $L_s = 48$. Symbols used as in Fig. 3, and the asterisk marks m_{res} . Solid line is a quenched chiral log fit to circles with $0.0 \leq m_f \leq 0.08$, and the dashed line is a linear fit to the same data.

jackknifing) decreases from 4.3 ± 2.6 to 3.6 ± 2.4 between the linear and logarithmic fits, it is not compelling enough to conclude firmly that the latter is preferable. On the other hand, our theoretical prejudice is for a fit which extrapolates to $(am_\pi)^2 = 0$ at $m_f = -m_{\text{res}}$.

The important conclusion from this study is that topological zero modes can contaminate quantities used to compute observables in small volume simulations. This interesting effect is a consequence of the index of the domain wall Dirac operator and, and it vanishes for increasing volume.

4. SCALING OF m_N/m_ρ

Vector meson and nucleon masses have been computed as functions of m_f on lattices at $\beta = 5.7, 5.85, \text{ and } 6.0$ on approximately equal spa-

tial volumes. Fig. 6a shows m_N/m_ρ vs. a^2 where the nucleon and rho masses have been extrapolated linearly to the chiral point $m_f = -m_{\text{res}}$. Although the scatter of the data points is only at the 1σ level, it is hard to draw a firm conclusion regarding their scaling behavior. The fit to $c_0 + c_2 a^2$ has a χ^2/dof of 2.4.

Given that the data for the pseudoscalar data hint at nonlinearities in the chiral extrapolations, one might wonder what role these would play in Fig. 6a. The smallest m_f in the $\beta = 5.7, 5.85,$ and 6.0 simulations correspond to $m_\pi/m_\rho = 0.38, 0.57,$ and $0.46,$ respectively. Therefore the different simulations would have different sensitivities to any deviation from linearity in the chiral limit. One way to test scaling while avoiding chiral extrapolation is to compare m_N/m_ρ at a value of m_π/m_ρ where simulations have been done. In Fig. 6b we plot m_N/m_ρ interpolating the data to $m_\pi/m_\rho = 0.61$. These data fit $c_0 + c_2 a^2$ with a χ^2/dof of 0.88.

5. STRANGE QUARK MASS

The calculation of the strange quark mass using this data was presented at DPF 2000 [7]. Using masses and matrix elements from [1] the strange quark mass is computed defined through both the vector and axial Ward-Takahashi identities (VWTI/AWTI). The renormalization factors are computed in the RI/MOM scheme [8,9]. We find at $\beta = 6.0$

$$m_s^{\overline{\text{MS}}}(2 \text{ GeV}) = \begin{cases} 110(2)(22) \text{ MeV} & \text{VWTI} \\ 105(6)(21) \text{ MeV} & \text{AWTI} \end{cases} \quad (4)$$

using the K mass to fix m_f for the strange sector. The first error is statistical, and the second is the systematic error due to using perturbation theory at 2 GeV to match to the $\overline{\text{MS}}$ scheme. At $\beta = 5.85$ we quote $m_s^{\overline{\text{MS}}}(2 \text{ GeV}) = 100(5)(20)$ MeV from the AWTI. Using the K^* instead to set $m_f^{(s)}$ increases $m_s^{\overline{\text{MS}}}(2 \text{ GeV})$ by $\approx 20\%$ at $\beta = 6.0$ and by $\approx 35\%$ at $\beta = 5.85$.

ACKNOWLEDGMENTS

Simulations performed with the RBRC and Columbia QCDSF's and the NERSC Cray T3E.

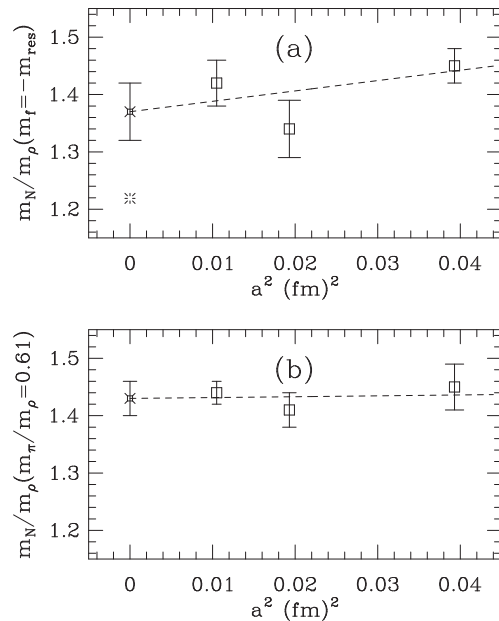


Figure 6. Nucleon–rho mass ratio on spatial volumes $\approx (1.6 \text{ fm})^3$. Squares denote domain wall results at $\beta = 6.0, 5.85,$ and 5.7 . The chiral limit $m_f + m_{\text{res}} \rightarrow 0$ has been taken in (a), and the asterisk marks the real world value. (b) shows m_N/m_ρ at $m_\pi/m_\rho = 0.61$. Dashed lines show fits to $c_0 + c_2 a^2$ and fancy squares the extrapolated $a = 0$ value.

REFERENCES

1. T. Blum *et al.*, hep-lat/0007038.
2. A. Ali Khan *et al.* [CP-PACS Collaboration], hep-lat/0007014.
3. G. T. Fleming *et al.*, Nucl. Phys. Proc. Suppl. **73**, 207 (1999).
4. A. Kaehler *et al.*, Nucl. Phys. Proc. Suppl. **73**, 405 (1999).
5. L. Wu, these proceedings.
6. S. R. Sharpe, Phys. Rev. **D46**, 3146 (1992).
7. M. Wingate, hep-lat/0009022.
8. C. Dawson, these proceedings.
9. T. Blum *et al.*, in preparation